

## High-Yield Singlet Fission in a Zeaxanthin Aggregate Observed by Picosecond Resonance Raman Spectroscopy

Chen Wang and Michael J. Tauber\*

Department of Chemistry and Biochemistry, University of California—San Diego, 9500 Gilman Drive MC 0314, La Jolla, California 92093-0314

Received April 5, 2010; E-mail: mtauber@ucsd.edu

**Abstract:** We report high-yield triplet generation by singlet fission upon photoexcitation of a new aggregate of the carotenoid all-*trans* 3*R*,3'*R*-zeaxanthin. The yield is determined by picosecond time-resolved resonance Raman spectroscopy, which allows direct characterization and quantification of triplet excited-state signatures and ground-state depletion. The technique and analysis reveals that triplets form within picoseconds. A quantum yield of 90–200% is derived with the assumption of weak exciton-coupling in the zeaxanthin aggregate.

The generation of multiple excitons upon absorption of a single photon has attracted attention recently, in part because of potential benefits to solar energy conversion.<sup>1,2</sup> Singlet fission, in which two triplet excited states are created from one singlet excited state, is a process that could significantly enhance the efficiency of organic molecular photovoltaics.<sup>3,4</sup> Fission plays a role in the photophysics of acenes,<sup>5–9</sup> polymers,<sup>10–12</sup> and other systems.<sup>13–15</sup> Correlations between triplet quantum yield (QY) and the relative energies of the lowest singlet and triplet states have been a primary focus.<sup>3</sup> However, investigations of the mechanism of intermolecular fission and the influence of fundamental properties such as the coupling strength and relative orientation of the interacting chromophores are rarely investigated.<sup>8</sup> Additionally, there are few reports of absolute triplet quantum yields from fission and even fewer where triplet signatures are directly monitored as part of the measurement. New approaches for time-resolved measurement of triplets and their yield must be employed to gain an improved understanding of the fission mechanism and to evaluate possible applications.

Here, we describe a new aggregate of the carotenoid all-*trans* 3*R*,3'*R*-zeaxanthin (Figure 1). Upon photoexcitation, we find direct evidence of intermolecular singlet fission by picosecond time-resolved resonance-Raman spectroscopy (TRRR). Zeaxanthin was selected principally because its excited states are expected to meet one criterion for efficient singlet fission: the T<sub>1</sub> excited state energy should be ~50% or less than the energy of the S<sub>1</sub> excited state.<sup>3,11</sup> Valence bond theory predicts that long polyenes meet this criterion;<sup>16</sup> experimentally, the S<sub>1</sub> energy of zeaxanthin is 14 500 cm<sup>-1</sup>, and the triplet energy is estimated to be 7000 ± 800 cm<sup>-1</sup>.<sup>16,17</sup> A second advantage of zeaxanthin is that it readily self-assembles in binary organic/aqueous solutions.<sup>18</sup> The aggregate studied here was prepared by adding water to a 100 μM solution of zeaxanthin in tetrahydrofuran (THF) to create a 90% (v/v) aqueous solution. Transmission electron microscopy (TEM) shows rod-shaped structures that are several hundreds of nanometers long and 20–30 nm wide (Figure 1). The TEM result is consistent with a broad probability distribution in hydrodynamic diameter (50–600 nm, with peak at 100 nm; Figure S2) determined by dynamic light scattering (DLS).

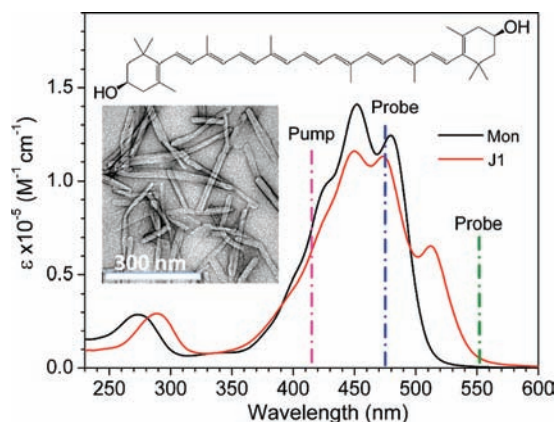


**Figure 1.** (Top) Molecular structure of 3*R*,3'*R*-zeaxanthin monomer, with UV-vis absorption spectrum in EtOH (black). The spectrum of the J1-aggregate in 90:10 H<sub>2</sub>O/THF is shown in red. Dashed lines indicate the 415 nm (pump) and 473 or 551 nm (probe) TRRR wavelengths. (Inset) TEM image of J1 aggregates.

A UV-vis absorption spectrum of the aggregate (Figure 1) has vibronic bands at 450, 474, and 512 nm which are within 2 nm of those reported for a J-aggregate of all-*trans* 3*R*,3'*R*-zeaxanthin diacetate.<sup>18</sup> A recent theoretical study on a closely related lutein diacetate aggregate has addressed the similarity of the monomer and aggregate absorption spectra, and the observed red shift is attributed to nonresonant dispersion interactions rather than a predominant J-type head-to-tail exciton coupling.<sup>19</sup> Nonetheless we denote the new aggregate J1 in keeping with the earlier literature and to distinguish it from a more red-shifted J-aggregate that was characterized in a recent ultrafast study.<sup>20</sup>

Continuous-wave (cw) resonance Raman spectroscopy shows nearly identical peak positions for the aggregate vs the monomer (Figure 2). Therefore the primary conclusion is that the molecular constituents in the aggregate are structurally similar to zeaxanthin monomers in solution, as found previously for other aggregates of zeaxanthin.<sup>21</sup> The aggregate shows slightly less Raman activity in the structurally sensitive C–H out-of-plane wagging modes at 874 and 967 cm<sup>-1</sup> (Figure 2, inset). This finding suggests that the molecules in the aggregate experience less structural distortion than in solution.<sup>15,22</sup> The 9 cm<sup>-1</sup> downshift for the ethylenic band of the aggregate is similar to other shifts for carotenoids in the solid state and has been attributed to crystal packing effects.<sup>22</sup>

TRRR was employed to distinguish and quantify excited state species. Samples were photoexcited at 415 nm and probed at 551 or 473 nm. A spectrum of the excited monomer in EtOH (Figure 3A) shows a highly upshifted ethylenic band at ~1790 cm<sup>-1</sup>, which is a signature of the S<sub>1</sub> excited state.<sup>23,24</sup> The S<sub>1</sub> decay and ground-state bleach recovery times are consistent with a ~10 ps lifetime for monomer β-carotene and zeaxanthin.<sup>25,26</sup> By contrast, the

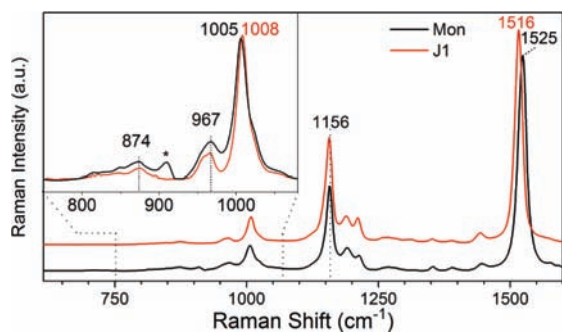


**Figure 2.** CW-resonance Raman spectra of zeaxanthin monomer in THF, and J1-aggregate in 90:10 H<sub>2</sub>O/THF excited with 458 nm. The spectra were normalized to equal peak heights of the ethylenic mode. (Inset) Magnified view of the fingerprint region. \* Residual peak from imperfect subtraction of THF solvent.

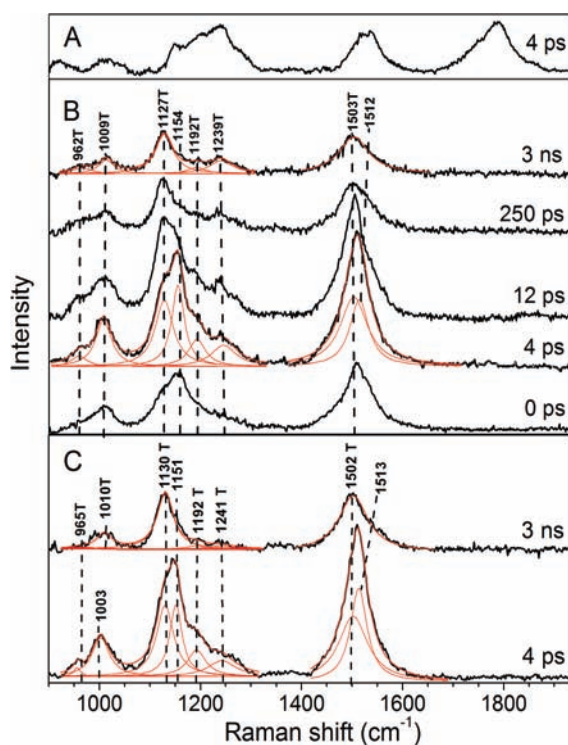


**Figure 3.** TRRR spectra of (A) monomer S<sub>1</sub> state, probed at 551 nm. (B) J1-aggregate in 90:10 H<sub>2</sub>O/THF probed at various delays between 415 nm pump and 551 nm probe. “T” indicates bands from the triplet state. (C) Same as (B) but probed with 473 nm.

resonance Raman spectra of the aggregate (Figure 3B, C) do not show S<sub>1</sub> features at the probe wavelengths of this study. Difference spectra acquired with a 551 nm probe at various delay times ranging from >20 ps to 3 ns are dominated by an ethylenic band peaked at 1503 cm<sup>-1</sup> and a band in the C–C fingerprint region peaked at 1127 cm<sup>-1</sup>. Additional bands in the fingerprint region have maxima at 1009, 1192, and 1239 cm<sup>-1</sup>. Spectra acquired with the 473 nm probe have nearly identical peak positions as those found with 551 nm (Figure 3C). Furthermore, the positions of the maxima are nearly identical to those of the triplet  $\beta$ -carotene monomer.<sup>27</sup> The frequencies of the long-lived species do not match those of carotenoid cation or anion radicals; thus charge separation is not supported.<sup>28,29</sup>

Significant evolution of the difference spectra is evident at pump–probe delay times from 0 ps to times later than 12 ps. The changes are analyzed by fitting the 4 ps spectra to a set of Lorentzian

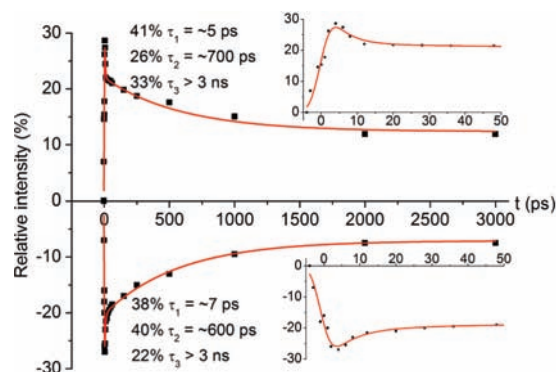


**Figure 4.** Relative Raman scattering intensity in the ethylenic band region. (Upper plot) Kinetics of positive ethylenic band intensity. (Lower plot) Kinetics of bleached ground state intensity centered at 1519 cm<sup>-1</sup>. The insets are magnifications at early times.

functions (Figure 3B, 3C). Short-lived bands centered at 1512 and ~1154 cm<sup>-1</sup> that do not coincide with the triplet bands are also apparent. To gain further insight into the dynamics of the system, we plot the integrated area of the ethylenic band growth and depletion at each time point (Figure 4). The points are fitted to a function which includes a 5.6 ps Gaussian instrument response and several variable exponential terms. The time constants that are found upon fitting are 5–7 ps, 600–700 ps, and >3 ns, in the proportions listed in Figure 4.

The kinetics and spectral analysis support the following picture: The triplet features appear at the earliest (0 ps) delay of pump and probe and reach a maximum within 4 ps. The ground state depletion at ~1519 cm<sup>-1</sup> reaches a minimum on a similar time scale. The rapid kinetics are consistent with triplet formation via an allowed singlet fission process. The precursor state is not seen but could be a hot S<sub>1</sub> state that is too short-lived to be detected. The prompt <10 ps decay of positive ethylenic intensity centered at 1503–1512 cm<sup>-1</sup> has two likely origins. First, prompt annihilation of triplets formed by singlet fission that do not diffuse apart can occur via T<sub>1</sub> + T<sub>1</sub> → S<sub>0</sub> (hot) + T<sub>2</sub>, in which the T<sub>2</sub> state is expected to quickly relax to T<sub>1</sub>. Second, vibrational cooling of hot S<sub>0</sub> produced by the annihilation can also cause the <10 ps decay. The bands at 1512 and 1154 cm<sup>-1</sup> are likely signatures of a hot S<sub>0</sub> state. The 600–700 ps kinetic component is attributed to triplets that escape immediate recombination and subsequently annihilate or decay back to the ground state. The existence of a >3 ns component supports the assignment of the long-lived species to a triplet state in the aggregate.

The analyses of triplet QYs depend upon quantification of the decreased scattering from the ground-state ethylenic band after photoexcitation. The depletion at 4 ps was measured for the monomer and aggregate samples as a function of percentage excitation (Figure 5). The percentage excitation is determined from Beer’s law, the pump energy, and the laser beam cross-sectional area. The ground-state depletion percentage is determined from the subtraction coefficient of a probe-only spectrum that gives the best removal of ground state from the pump + probe spectra (see Supporting Information (SI)). Both the monomer and aggregate show linear depletion up to the 20% excitation ratio explored here. It is significant that the extent of depletion for the aggregate at these powers is twice that of the monomer, and within experimental error the slopes of the lines in Figure 5 have a ratio of 2:1. There are two possible explanations for this result. First, one would expect the depletion of two chromophores per absorbed photon in the case of highly efficient intermolecular singlet fission. If annihilation occurred after fission, the bleach would still remain, as long as the

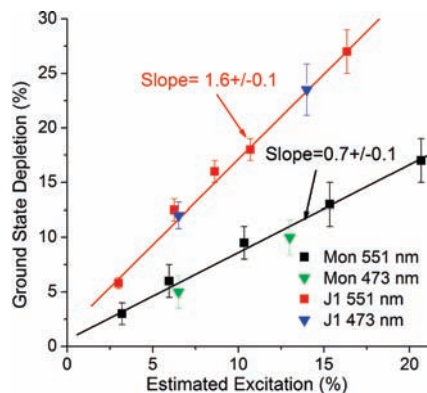


**Figure 5.** Percentage of ground state depletion for 415 nm photoexcitation, with varying pump energies at 4 ps time delay. The excitation % is determined from spot size measurements and laser pulse energy; the depletion is determined from difference spectra.

hot  $S_0$  ethylenic frequency is significantly shifted from the parent ground state frequency at  $1519\text{ cm}^{-1}$ . Thus the 2-fold greater slope for the J1-aggregate is indirect evidence for a  $\sim 200\%$  triplet yield, i.e. quantitative intermolecular singlet fission.

A second possible origin of a 2-fold greater magnitude for the depletion of the aggregate is that the transition dipole of exciton-coupled systems is theoretically expected to scale as  $(N_{\text{coh}})^{0.5}$ , where  $N_{\text{coh}}$  is the number of coherently coupled molecules in the exciton state.<sup>30</sup> Therefore, the TRRR transient bleach signals of the exciton-coupled zeaxanthin aggregate could be enhanced relative to the monomer signal by a factor of  $(N_{\text{coh}})^2$ , since four interactions with the pump and probe fields are involved. Enhancements of this kind have been discussed for pump–probe transient absorption spectroscopy of strongly coupled J-aggregates of pseudoisocyanine (PIC) dyes.<sup>30</sup> However, we consider this possibility unlikely in the case of J1-zeaxanthin for two reasons. First, the cross section per molecule (Figure 1) closely corresponds to the monomer cross section in most spectral regions, and particularly at the 415 nm pump wavelength; thus the J1-zeaxanthin is qualitatively different from PIC in this regard. Second, the QY result for J1 is independent of whether the probe is resonant with the 473 nm monomeric region or significantly red-shifted to 551 nm. Together the two factors suggest that the zeaxanthin J1-aggregate is weakly exciton-coupled<sup>19</sup> and can be treated as if  $N_{\text{coh}} \approx 1$ . In that case, the pump pulse in our experiments is a linear actinic pulse for  $<20\%$  excitation.

A second approach for analyzing the triplet QY incorporates the triplet excited-state band area along with the ground state depletion (see SI). First the ratio of the triplet and ground state resonance Raman cross sections is found from the percentage of ground state depletion and the ratio of triplet/ground state ethylenic band intensities at 3 ns. Next, the percentage of molecules in the triplet excited state can be determined at the 4 ps pump–probe delay, assuming that (1) the triplet cross section remains the same at 4 ps as for 3 ns and (2) the area of the  $1503\text{ cm}^{-1}$  Lorentzian band is a good indicator of triplet population. When the percentage of triplets is divided by the excitation ratio the resulting triplet QY at 4 ps is  $\sim 90\%$  per absorbed photon, at the lowest pump energy. Similar results are obtained for either 473 or 551 nm probe. The 90% estimate is obviously lowered by any annihilation that causes loss of scattering intensity at  $1503\text{ cm}^{-1}$  during the 4 ps delay. Without annihilation, the direct triplet yield could reach the  $\sim 200\%$  found by examination of ground-state depletion (i.e., slopes of Figure 5).

Triplet yields as high as 30% by singlet fission have been reported in carotenoids of light harvesting centers.<sup>15,31</sup> However in these

systems the absence of proximal carotenoids rules out the possibility of intermolecular homofission. Instead, the recent reports support an intramolecular fission mechanism which is enhanced by distortion of the carotenoid.<sup>15,32,33</sup> An alternative mechanism is singlet heterofission between a carotenoid and nearby bacteriochlorophyll molecule.<sup>31</sup> By contrast, the aggregate of the present study consists of undistorted carotenoid molecules, and exhibits a higher triplet QY than the light harvesting systems.

In summary, picosecond TRRR is found to be a powerful tool for identifying and quantifying the triplet yields in a self-assembled carotenoid aggregate. The spectra reveal that the J1-aggregate of zeaxanthin forms triplets in  $<4\text{ ps}$  by a highly efficient intermolecular singlet fission process, possibly via a short-lived hot  $S_1$  state. The triplet QY of 90–200% derived assuming weak coupling is remarkable in view of the 0.2% triplet QY for monomeric zeaxanthin.<sup>34</sup> The influence of aggregate structure on QY and further investigation of the exciton coherence number are aims of ongoing experiments which will be reported elsewhere.

**Acknowledgment.** Acknowledgment is made to the donors of the ACS-Petroleum Research Fund, and to the Hellman Family Foundation, for partial support of this research. We thank Brittany Merrill for help in the preparation of the aggregate; Norm Olson and Miaoping Chien for assistance with TEM; and Prof. Frederick Khachik for a reference NMR spectrum of 3R,3'R-zeaxanthin.

**Supporting Information Available:** DLS data; NMR, CD spectra; TEM procedure; Description of TRRR spectrometer; TRRR workup procedure, spectra of monomer, further detail on QY analysis. This material is available free of charge via the Internet at <http://pubs.acs.org>.

## References

- (1) Nozik, A. J. *Chem. Phys. Lett.* **2008**, *457*, 3–11.
- (2) McGuire, J. A.; Joo, J.; Pietryga, J. M.; Schaller, R. D.; Klimov, V. I. *Acc. Chem. Res.* **2008**, *41*, 1810–1819.
- (3) Paci, I.; Johnson, J. C.; Chen, X. D.; Rana, G.; Popović, D.; David, D. E.; Nozik, A. J.; Ratner, M. A.; Michl, J. *J. Am. Chem. Soc.* **2006**, *128*, 16546–16553.
- (4) Schwerin, A. F.; et al. *J. Phys. Chem. A* **2010**, *114*, 1457–1473.
- (5) Singh, S.; Jones, W. J.; Siebrand, W.; Stoeicheff, B. P.; Schneider, W. G. *J. Chem. Phys.* **1965**, *42*, 330–342.
- (6) Swenberg, C. E.; Geacintov, N. E. In *Organic Molecular Photophysics*; Birks, J. B., Ed.; John Wiley & Sons: London, 1973; Vol. 1, pp 489–564.
- (7) Jundt, C.; Klein, G.; Sipp, B.; Le Moigne, J.; Joucla, M.; Villaeys, A. A. *Chem. Phys. Lett.* **1995**, *241*, 84–88.
- (8) Müller, A. M.; Avlasevich, Y. S.; Schoeller, W. W.; Müllen, K.; Bardeen, C. J. *J. Am. Chem. Soc.* **2007**, *129*, 14240–14250.
- (9) Thørsmolle, V. K.; Averitt, R. D.; Demisar, J.; Smith, D. L.; Tretiak, S.; Martin, R. L.; Chi, X.; Crone, B. K.; Ramirez, A. P.; Taylor, A. J. *Phys. Rev. Lett.* **2009**, *102*, 017401.
- (10) Kraebel, B.; Hulin, D.; Aslangul, C.; Lapersonne-Meyer, C.; Schott, M. *Chem. Phys.* **1998**, *227*, 83–98.
- (11) Österbacka, R.; Wohlgenannt, M.; Shkunov, M.; Chinn, D.; Vardeny, Z. V. *J. Chem. Phys.* **2003**, *118*, 8905–8916.
- (12) Lanzani, G.; Stagira, S.; Cerullo, G.; De Silvestri, S.; Comoretto, D.; Moggio, I.; Cuniberti, C.; Musso, G. F.; Dellepiane, G. *Chem. Phys. Lett.* **1999**, *313*, 525–532.
- (13) Agostini, G.; Corvaja, C.; Giacometti, G.; Pasimeni, L. *Chem. Phys.* **1993**, *173*, 177–186.
- (14) Watanabe, S.; Furube, A.; Katoh, R. *J. Phys. Chem. A* **2006**, *110*, 10173–10178.
- (15) Papagiannakis, E.; Das, S. K.; Gall, A.; van Stokkum, I. H. M.; Robert, B.; van Grondelle, R.; Frank, H. A.; Kennis, J. T. M. *J. Phys. Chem. B* **2003**, *107*, 5642–5649.
- (16) Christensen, R. L. In *The Photochemistry of the Carotenoids*; Frank, H. A., Young, A. J., Britton, G., Cogdell, R. J., Eds.; Kluwer Academic Publishers: Dordrecht, 1999; Vol. 8, pp 137–157.
- (17) Josue, J. S.; Frank, H. A. *J. Phys. Chem. A* **2002**, *106*, 4815–4824.
- (18) Zsila, F.; Bikádi, Z.; Deli, J.; Simonyi, M. *Chirality* **2001**, *13*, 446–453.
- (19) Spano, F. C. *J. Am. Chem. Soc.* **2009**, *131*, 4267–4278.
- (20) Billsten, H. H.; Sundström, V.; Polívka, T. *J. Phys. Chem. A* **2005**, *109*, 1521–1529.
- (21) Salares, V. R.; Young, N. M.; Carey, P. R.; Bernstein, H. J. *J. Raman Spectrosc.* **1977**, *6*, 282–288.
- (22) Saito, S.; Tasumi, M.; Eugster, C. H. *J. Raman Spectrosc.* **1983**, *14*, 299–309.
- (23) Orlandi, G.; Zerbetto, F.; Zgierski, M. Z. *Chem. Rev.* **1991**, *91*, 867–891.



- (24) McCamant, D. W.; Kukura, P.; Mathies, R. A. *J. Phys. Chem. A* **2003**, *107*, 8208–8214.
- (25) Wasielewski, M. R.; Kispert, L. D. *Chem. Phys. Lett.* **1986**, *128*, 238–243.
- (26) Polívka, T.; Sundström, V. *Chem. Rev.* **2004**, *104*, 2021–2071.
- (27) Hashimoto, H.; Koyama, Y. *J. Phys. Chem.* **1988**, *92*, 2101–2108.
- (28) Jeevarajan, A. S.; Kispert, L. D.; Chumanov, G.; Zhou, C.; Cotton, T. M. *Chem. Phys. Lett.* **1996**, *259*, 515–522.
- (29) Jin-Yeol, K.; Furukawa, Y.; Tasumi, M. *Chem. Phys. Lett.* **1997**, *276*, 418–422.
- (30) Knoester, J.; Spano, F. In *J-Aggregates*; Kobayashi, T., Ed.; World Scientific Publishing Co.: Singapore, 1996; pp 111–160.
- (31) Angerhofer, A. In *The Photochemistry of the Carotenoids*; Frank, H. A., Young, A. J., Britton, G., Cogdell, R. J., Eds.; 1999, pp 203–222.
- (32) Gradinaru, C. C.; Kennis, J. T. M.; Papagiannakis, E.; van Stokkum, I. H. M.; Cogdell, R. J.; Fleming, G. R.; Niederman, R. A.; van Grondelle, R. *Proc. Natl. Acad. Sci. U.S.A.* **2001**, *98*, 2364–2369.
- (33) Tavan, P.; Schulten, K. *Phys. Rev. B* **1987**, *36*, 4337–4358.
- (34) Nielsen, B. R.; Jørgensen, K.; Skibsted, L. H. *J. Photochem. Photobiol. A: Chem.* **1998**, *112*, 127–133.

JA102851M